IEEE Access
Multidisciplinary | Rapid Review | Open Access Journal

Received December 29, 2017, accepted February 5, 2018, date of publication February 14, 2018, date of current version March 13, 2018.

Digital Object Identifier 10.1109/ACCESS.2018.2805883

Design and Comparison of Fuel-Saving Speed Planning Algorithms for Automated Vehicles

SHAOBING XU AND HUEI PENG
Department of Mechanical Engineering, University of Michigan, Ann Arbor, MI 48109, USA
Corresponding author: Huei Peng (hpeng@umich.edu)

This work was supported by the Open Connected and Automated Vehicle Project of Mcity.

ABSTRACT Intelligent planning and accurate execution of connected automated vehicles (CAVs) enable not only improved traffic safety but also better fuel economy. This paper presents two longitudinal speed planning algorithms for fuel-saving driving on highways with varying road slopes. One is designed on the top of the model predictive control (MPC) and the other is called equivalent kinetic-energy and fuel conversion method. The MPC algorithm solves the optimal speed profile in a receding finite horizon with repeated optimization, which is numerically solved by the Legendre pseudospectral method. The latter is designed based on an instantaneous optimization, which considers vehicle kinetic energy an admissible power source, and then minimizes a weighted sum of fuel energy and kinetic energy. This strategy is capable of generating analytical rules to get the economical speed as well as the corresponding commands of the engine, transmission, and brake. The two algorithms are featured by near-global optimization and local optimization, respectively. Their performances in fuel economy and computational load are quantitatively explored and compared in order to distinguish the potential of real implementation in CAVs.

INDEX TERMS Automated vehicles, speed planning, vehicle dynamics control, eco-driving.

I. INTRODUCTION

A. MOTIVATION

Connected and automated vehicles (CAVs) are gradually penetrating into the real-world traffic system, and able to enhance traffic safety, liberate human drivers who are unfit or do not want to drive, and also improve fuel economy [1]. The fuel consumption of a CAV is dominated by powertrain efficiency, but significantly affected by the speed planning and control strategies [2]. They are usually related to the fuel-efficient speed automation, which explores the speed flexibility to improve system efficiency [3].

Fuel-saving speed planning techniques were estimated to have the potential of reducing fuel consumption by up to 15% [4], [5]. This potential is attractive compared to the converged improvements in internal combustion engine efficiency, and even approaches the capacity of hybrid powertrains. The fuel-saving speed planning can be developed for various scenarios, e.g., driving through signalized intersections with economical responses to traffic lights [7], [8]. This paper focuses on the scenario of highway driving, in which the lead vehicle's states and road slope signal can be collected by connection technologies and digital map, then the speed profile is optimized to save fuel by avoiding inefficient engine operations and unnecessary idling/braking [9], [10].

When driving on the real-world highways, the road slope and lead vehicle deliver essentially different effects on the speed planning due to the fact that, the road slope profile is determinate while the lead vehicle is dynamically changing with uncertain behaviors. This uncertainty requires dynamic speed adaption/planning in real time. To reconcile the different features, one strategy is to merge all factors into a model predictive control (MPC) framework, and try to solve the nonlinear optimization problem online with heavy computing load; examples can be found in [10] and [11]. However, we tend to apply the concept of two-hierarchy speed planning strategy reported in [12], which separated the determinate and uncertain factors into different hierarchies. In detail, the upper hierarchy mainly considers the determinate road slope to generate a fuel-saving reference speed trajectory, and the lower-hierarchy then adjusts it according to the surrounding vehicles.

In congested traffic flow, the lower-hierarchy (or lead vehicle) dominates speed trajectory and the road slope has little effect, where the adaptive cruising control (ACC) system may be adopted. It can follow a lead vehicle, but has a fixed

predefined reference speed and treats the road slope as a disturbance [13]. On the contrary, in the sparse traffic flow, the road slope dominates the fuel-saving speed level, even though the lead vehicle may occasionally intervene. The fuel-saving driving resembles the conventional cruising control (CC), but the difference is that the vehicle speed can adapt to road slope instead of maintaining a constant set by drivers randomly. For automated vehicles or the ACC system, the adaption to lead vehicles has been well addressed and commercialized, while the fuel-efficient slope adaption is still absent. Therefore, this paper focuses on developing fuel-saving speed planning algorithms that can adapt to road slopes for CAVs; the resulted speed profile can also be used as the reference speed of CC/ACC systems to replace the fixed settings.

B. SPEED PLANNING WITH ROAD SLOPES

The knowledge about road slope is important to achieve better fuel economy since this major disturbance significantly affects the driving load, vehicle speed, and actuator operations. When planning speed on varying slopes, synergistic optimization of the engine, transmission, and brake system is required to improve the overall system efficiency [10]. Human drivers can naturally optimize control actions to adapt to the terrain with perceiving the upcoming slopes. For automated vehicles, the optimization and the adaptation to road slope typically can be achieved through the aforementioned MPC [11]. It generates the optimal speed and control actions over a finite horizon and is able to deal with the future road shape as well as system constraints. For example, the MPC method developed by Kamal *et al.* [14] obtained about 5% fuel reduction compared to a constant-speed driving. Hellström *et al.* [10] studied the tradeoff between fuel consumption and trip time in a look-ahead control framework for heavy trucks. Due to the time-varying uncertainty, both the surrounding vehicles and traffic lights were not considered in these two studies. The major imperfection of these optimization-based systems is that they usually involved in strong nonlinearity arising from the engine, powertrain, and road slope, which thus ends up with heavy computation load [15].

As an alternative to the near-global optimization-based MPC method, another strategy is to shorten the predictive horizon and even uses the instantaneous slope information and vehicle states to generate the proper speed level, called non-predictive or local-optimization based method. A well-known non-predictive method is the equivalent consumption minimization strategy (ECMS), an energy management algorithm for hybrid vehicles, which optimizes the power allocation between engine and motor considering only the current vehicle states and the input speed. This method dramatically reduced computational load and achieved fuel economy only slightly worse than the global optimization results [16]. For vehicle speed planning, Schwarzkopf and Leipni [9] developed a non-predictive eco-cruising algorithm by simplifying the dynamic Hamiltonian system , i.e., using a fixed co-state to replace the dynamic one. This algorithm allowed for real-time implementation, while the fuel-saving capacity was not discussed. Xu *et al.* [17] also proposed the concept of instantaneous feedback cruising controls to fast respond to road slope and lead vehicles.

Both the near-global optimization based MPC strategies and the non-predictive methods have potentialities to be applied to fuel-saving speed planning. Generally, when applying a speed planning algorithm to a CAV with limited computation capability, both fuel economy and computation efficiency should be considered and even compromised. This fact requires further insights into the different properties between the two types of methods.

C. CONTRIBUTIONS

The objective of this paper is to explore the design theory and different natures of near-global and local optimization based speed planning algorithms, in order to understand the efficient strategy to generate fuel-saving speed trajectories for CAVs or CC/ACC systems. The contributions include: 1) a nonlinear fuel-minimized MPC algorithm is developed; the optimal solution at each step is solved by the Legendre pseudo-spectral method; 2) a local optimization based algorithm called equivalent kinetic energy and fuel conversion (EKFC) is designed to generate the proper speed level and the commands of throttle, brake, and transmission; 3) their performances in fuel economy and computation load are quantitatively analyzed and compared. Mechanism of the different performances is then qualitatively discussed.

The remainder of this paper is organized as follows: Section II presents the problem formulation; Section III and IV design the MPC and EKFC algorithms, respectively; their performance is shown in Section V; Section VI discusses their different natures; and Section VII concludes this paper.

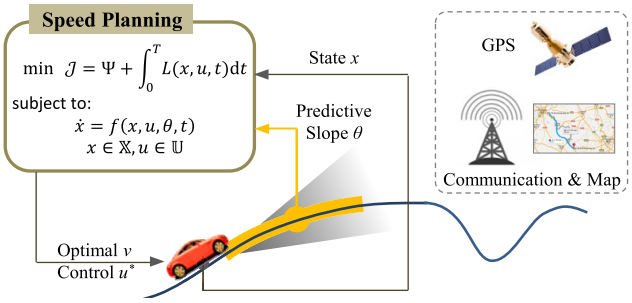

FIGURE 1. Concept of fuel-saving speed planning for connected and automated vehicles.

II. FORMULATION OF FUEL-SAVING SPEED PLANNING PROBLEM

The concept of fuel-saving speed planning on varying terrain is shown in Fig. 1. The CAV can collect road slope information from a digital map or wireless communication. The speed planning algorithm then optimizes the vehicle

motion considering the powertrain characteristics, including the engine efficiency, transmission gear, and braking energy. The effects of lead vehicles will not be considered in this paper, as explained in the introductory section. In this section, we present the vehicle longitudinal dynamics model and then formulate the speed planning problem.

A. VEHICLE LONGITUDINAL DYNAMICS MODEL

The studied vehicle is equipped with a 2.0-liter internal combustion engine (ICE) and a 5-speed automated manual transmission (AMT). To simplify speed planning, the following assumptions are made: (i) the dynamics of transmission is ignored, including the gear-shifting transients; (ii) the mechanical efficiency of powertrain is a constant regardless of gear position and power level. Then the simplified longitudinal dynamics is modeled as

$$\begin{aligned} \dot{s} &= v \\ M\dot{v} &= \frac{\eta_{\mathrm{T}}\mathcal{P}_{\mathrm{e}}}{v} + \mathcal{B} - C_A v^2 - \mathcal{F}_R(s) \\ \mathcal{P}_{\mathrm{e}} &= \omega_{\mathrm{e}} T_{\mathrm{e}} \\ \mathcal{F}_R(s) &= Mg\left(f\cos\theta\left(s\right) + \sin\theta\left(s\right)\right) \end{aligned} \tag{1}$$

where s and v are the vehicle position and speed; M is the vehicle mass; η_{T} is the overall powertrain efficiency; $\mathcal{P}_{\mathrm{e}}$ is the engine output power; $\mathcal{B}$ is the braking force, including the engine drag torque; C_A is the aerodynamic drag coefficient; ω_{e} and T_{e} are the engine speed and torque; $\mathcal{F}_R$ denotes the rolling resistance and gravity resistance; f is the rolling resistance coefficient; and $\theta\left(s\right)$ is the road slope, which is a function of distance s.

The engine speed ω_{e} and vehicle speed v are governed by

$$\omega_{\mathrm{e}} = k_\omega v i_{\mathrm{g}} \tag{2}$$

where k_ω is the lumped coefficient; i_{g} is the discrete gear ratio of AMT,

$$i_{\mathrm{g}} \in \mathbb{I} = \left\{i_{\mathrm{g}1}, i_{\mathrm{g}2}, i_{\mathrm{g}3}, i_{\mathrm{g}4}, i_{\mathrm{g}5}\right\} \tag{3}$$

In addition, the engine and brake system are constrained by their physical limits:

$$\mathbb{C}_{\mathrm{pl}} = \left\{ \begin{array}{c} \omega_{\min} \le \omega_{\mathrm{e}} \le \omega_{\max} \\ 0 \le T_{\mathrm{e}} \le T_{\max}\left(\omega_{\mathrm{e}}\right) \\ 0 \le \mathcal{P}_{\mathrm{e}} \le \mathcal{P}_{\max} \\ \mathcal{B}_{\lim} \le \mathcal{B} < 0 \end{array} \right\} \tag{4}$$

The maximum engine torque $T_{\max}$ is modeled by a 4^{th}-order polynomial of ω_{e},

$$T_{\max}\left(\omega_{\mathrm{e}}\right) = \sum\nolimits_{i=0}^{4} \kappa_{\mathrm{m},i}\, \omega_{\mathrm{e}}^{i} \tag{5}$$

To establish a direct mapping between vehicle speed and traveling distance, the dynamics (1) is converted into the spatial domain when $v > 0$, i.e.,

$$\frac{\mathrm{d}v}{\mathrm{d}s} = \frac{1}{v}\dot{v}\left(\mathcal{P}_{\mathrm{e}}, \mathcal{B}, s\right) \tag{6}$$

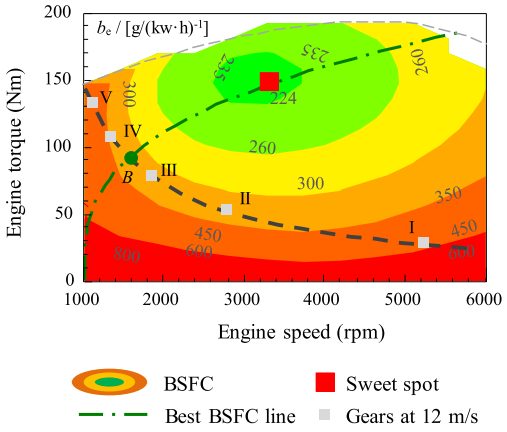

FIGURE 2. Engine brake specific fuel consumption (BSFC) map. The best BSFC line is fitted as the green dash-dot curve; the red square point stands for the sweet spot, located at ω_{e}= 3150 rpm and T_{e}= 150 Nm; the thick dotted line stands for the equal-power curve of 15 kW; the small square points indicate the admissible engine operating points with different AMT gears at 12 m/s.

An engine efficiency map is used to estimate the fuel consumption. The fueling rate $\mathcal{Q}_{\mathrm{e}}$ depends on engine power $\mathcal{P}_{\mathrm{e}}$ and efficiency, i.e.,

$$\mathcal{Q}_{\mathrm{e}}\left(T_{\mathrm{e}}, \omega_{\mathrm{e}}\right) = g\left(T_{\mathrm{e}}, \omega_{\mathrm{e}}\right) \cdot \mathcal{P}_{\mathrm{e}} \tag{7}$$

where g stands for the brake specific fuel consumption (BSFC) as shown in Fig. 2. The best BSFC line, a collection of points with the highest engine efficiency at fixed power levels, is marked by the dash-dot line. If the engine always operates on this line, the fueling rate then depends on engine power only and can be estimated by the VT-CPFM1 model [18], i.e.,

$$\mathcal{Q}_{\mathrm{e}}\left(\mathcal{P}_{\mathrm{e}}\right) = \kappa_0 + \kappa_1 \mathcal{P}_{\mathrm{e}} + \kappa_2 \mathcal{P}_{\mathrm{e}}^2, \quad \mathcal{P}_{\mathrm{e}} \ge 0 \tag{8}$$

In this paper, the simplified model (8) is used for the design of speed planning algorithms only, and the map-based model (7) is adopted to estimate the real fuel consumption in simulations. The key parameters of the engine model and vehicle dynamics are listed in Table 1.

TABLE 1. Key parameters of the vehicle model.

Parameter	Value	Parameter	Value
M	1600 kg	$\omega_{\max}$	6000 rpm
η_{T}	0.90	$\mathcal{B}_{\lim}$	-6000 N
C_A	0.43	κ_0	3.048 g/s
f	0.028	κ_1	0.0905 g/(s·kW),
k_ω	120.16	κ_2	0.00148 g/(s·kW^2)
$\omega_{\min}$	1000 rpm		
i_{g}	3.620, 1.925, 1.285, 0.933, 0.692		

B. FUEL-OPTIMAL SPEED PLANNING PROBLEM

The fuel-saving speed planning is formulated as an optimal control problem (OCP) with the objective J minimizing

engine fuel consumption, defined as

$$\min \mathcal{J} = \int_{s_0}^{s_f} \frac{\mathcal{Q}_e}{v} \mathrm{d}s \tag{9}$$

where s_0 and s_f are the initial and final distance.

Considering the speed limits in real traffic system, a hard constraint is imposed on v, i.e.,

$$v_{\min} \le v \le v_{\max} \tag{10}$$

Note that even though the trip time is not constrained in this fuel-oriented system, one can regulate the speed constraint to achieve an acceptable trip time.

With the aforementioned vehicle model and cost function, the fuel-optimal speed planning problem is formulated as

$$\begin{aligned} \min \mathcal{J} &= \int_{s0}^{sf} \frac{\mathcal{Q}_e}{v} \mathrm{d}s \\ s.t.\ \frac{\mathrm{d}v}{\mathrm{d}s} &= \frac{1}{vM}\left(\frac{\eta_T \mathcal{P}_e}{v} + \mathcal{B} - C_A v^2 - \mathcal{F}_R(s)\right) \\ & v_{\min} \le v \le v_{\max} \\ & \omega_e, T_e, \mathcal{P}_e, \mathcal{B} \in \mathbb{C}_{pl} \\ & i_g \in \mathbb{I} \end{aligned} \tag{11}$$

The system states are vehicle speed v and distance s, denoted by $\boldsymbol{x} = (v, s)^T$; the control inputs include engine power $\mathcal{P}_e$, brake force $\mathcal{B}$, and transmission gear i_g, denoted by $\boldsymbol{u} = \left(\mathcal{P}_e, \mathcal{B}, i_g\right)^T$. Due to the discontinuity of AMT gear ratio i_g and the nonlinearity in vehicle dynamics and engine fuel model, the formulated problem is a typical nonlinear mixed-integer OCP with an unknown switching structure of i_g. In the following subsection, a rule-based AMT control strategy is proposed to simplify the optimization.

C. TRANSMISSION CONTROL STRATEGY

Assuming that the vehicle is equipped with an ideal continuously variable transmission (CVT), then the engine can always operate on the best BSFC line by dynamically manipulating the gear ratio of CVT [6]. The equipped AMT of the studied vehicle, however, can only select one of the five gears at a given speed level, e.g., the point I to V in Fig. 2 at 12 m/s. To avoid solving the mixed-integer optimization directly, we first assume that the gear ratio of AMT is continuous as an ideal CVT; then the original problem becomes a continuous-state OCP and can be solved with reduced complexity. Once the speed profile, engine power, and gear ratio of the ideal CVT are optimized, the real gear of AMT is determined by the following principle: the gear position is selected to maximize engine efficiency η_e under the optimized engine power P_e^* (e.g., gear III in Fig. 2), i.e.,

$$i_g^* = \arg\max_{i_g \in \mathbb{I}} \left\{ \eta_e\left(\omega_e, T_e\right) \mid \omega_e = k_\omega v i_g, T_e = \mathcal{P}_e^* / \omega_e \right\} \tag{12}$$

This rule is capable of selecting a near-optimal feasible AMT gear, which is actually closest to the optimized gear ratio of the ideal CVT. An example is shown in Fig. 3, in which the AMT tracks the continuous trajectory solved from the ideal CVT. Generally, this control strategy enables the engine to run near the best BSFC line and can achieve near-optimal performance, even though the discrete gears may weaken fuel economy by about 3% compared to the ideal CVT.

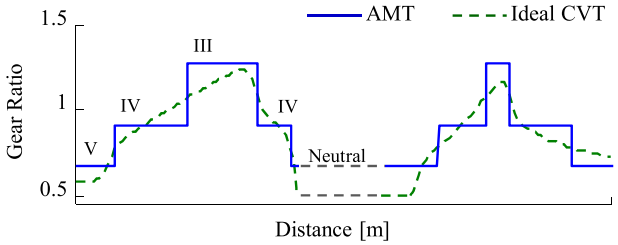

FIGURE 3. Gear selection of AMT using discrete gear ratios to approach the operation of CVT.

III. ALGORITHM DESIGN OF MODEL PREDICTIVE CONTROL

For the formulated problem (11), a straightforward method is to numerically solve it by global optimization over the whole horizon. It is suitable for tasks with short mileages but becomes less practicable for long mileage (e.g., 50 km) because the dimensions of the discretized problem will be over high. In this section, we adopt the receding horizon optimization to solve the fuel-saving speed profile, called MPC method. It is based on iterative, near-global horizon optimization of a plant model and is able to achieve near-optimal performance [10], [14].

We design the MPC problem from the original OCP (11) with a shortened fixed predictive horizon s_T, i.e.,

$$\begin{aligned} \min \mathcal{J} &= \int_{s_n}^{s_n+s_T} \frac{\mathcal{Q}_e\left(\mathcal{P}_e\right) + \beta\left(v - \bar{v}\right)^2}{v} \mathrm{d}s \\ s.t.\ \frac{\mathrm{d}v}{\mathrm{d}s} &= \frac{1}{vM}\left(\frac{\eta_T \mathcal{P}_e}{v} + \mathcal{B} - C_A v^2 - \mathcal{F}_R(s)\right) \\ & v_{\min} \le v \le v_{\max} \\ & \mathcal{P}_e, \mathcal{B} \in \mathbb{C}_{pl} \\ & s_n = n \cdot \Delta s, \quad n = 0, 1, 2 \cdots \end{aligned} \tag{13}$$

where s_n is the initial position at the n^{th} step; Δs is the step length. A penalty term $\beta\left(v - \bar{v}\right)^2$ is introduced to avoid that the speed drops to zero to get the lowest fuel consumption in the predictive horizon; the average speed $\bar{v}$ is set based on a roughly estimated trip time [14]. By solving problem (13), the optimal speed profile, engine power $\mathcal{P}_e^*$ and brake force $\mathcal{B}^*$ in $[s_n, s_n + s_T]$ are obtained, and the used control input $\boldsymbol{u}_n^*(s)$ in $[s_n, s_{n+1}]$ is set to

$$\boldsymbol{u}_n^*(s) = \left[\mathcal{P}_e^*\left(s_n\right), B^*\left(s_n\right)\right]^T s \in [s_n, s_{n+1}] \tag{14}$$

Note that the speed planning methods designed in this paper not only output the optimal speed trajectory but also generate control commands of gear, throttle and brake, in order to decouple the fuel economy from other servo-loop speed tracking controllers (e.g., PID).

To solve the nonlinear MPC problem (13) efficiently, the Legendre pseudo-spectral method (LPM) is applied to the numerical optimization in this paper [19]. The LPM is a global collocation algorithm for converting OCP into a nonlinear programming (NLP) problem [19], [20]. Compared to the conventional methods (e.g., shooting method), it discretizes the OCP at orthogonal collocation points and then employs global interpolating polynomials to approximate states and control inputs, which thus allows for better accuracy and convergence speed [20].

To convert the problem (13) into an NLP, the LPM adopts the Legendre–Gauss–Lobatto (LGL) collocation points for discretization, which are the roots of the derivative of $\mathcal{N}^{\text{th}}$ order Legendre polynomial $P_{\mathcal{N}}$, together with two end points -1 and 1, denoted as $\tau_i \in [-1, 1]$, $i = 0, 1, \cdots, \mathcal{N}$. The predictive horizon is transformed to a canonical interval $[-1, 1]$ by

$$\tau = \frac{2s - (2s_n + s_{\mathrm{T}})}{s_{\mathrm{T}}} \tag{15}$$

The engine power $\mathcal{P}_{\mathrm{e}}$, brake force $\mathcal{B}$, vehicle speed v and distance s are discretized to $\mathbb{P}_i$, $\mathbb{B}_i$, $\mathbb{V}_i$ and $\mathbb{S}_i$, respectively. The dynamic states and control inputs are approached by the Lagrange interpolation at collocation points, for instance,

$$\mathcal{P}_{\mathrm{e}}(\tau) \approx \sum\nolimits_{i=0}^{\mathcal{N}} l_i(\tau)\, \mathbb{P}_i \tag{16}$$

where $\ell_i(\tau)$ is the Lagrange basis polynomial.

The differential state equation can be approximated by the differential operation on the Lagrange basis polynomials. Then the vehicle dynamics (6) is converted to a series of equality constraints at the collocation points, i.e.,

$$\sum\nolimits_{i=0}^{\mathcal{N}} D_{ki}\mathbb{V}_i = \frac{s_{\mathrm{T}}}{2\mathbb{V}_k M}\left(\frac{\eta_{\mathrm{T}}\mathbb{P}_k}{\mathbb{V}_k} + \mathbb{B}_k - C_A\mathbb{V}_k^2 - \mathcal{F}_R(\mathbb{S}_k)\right) \tag{17}$$

where $k = 0, 1, 2, \cdots, \mathcal{N}$, and D_{ki} is the differentiation matrix with explicit expression [20]:

$$D_{ki} = \begin{cases} \dfrac{P_{\mathcal{N}}(\tau_k)}{P_{\mathcal{N}}(\tau_i)(\tau_k - \tau_i)} & i \neq k \\ -\mathcal{N}(\mathcal{N}+1)/4 & i = k = 0 \\ \mathcal{N}(\mathcal{N}+1)/4 & i = k = \mathcal{N} \\ 0 & \text{otherwise} \end{cases} \tag{18}$$

The cost function is computed by the Gaussian-Lobatto quadrature, i.e.,

$$\min \mathcal{J} = \frac{s_{\mathrm{T}}}{2}\sum\nolimits_{k=0}^{\mathcal{N}} \frac{w_k\left(\mathcal{Q}_{\mathrm{e}}(\mathbb{P}_k) + \beta(\mathbb{V}_k - v_{\mathrm{d}})^2\right)}{\mathbb{V}_k} \tag{19}$$

where w_k is the integral weight defined as

$$w_k = \int_{-1}^{1} \ell_k(\tau)\mathrm{d}\tau = \frac{2}{\mathcal{N}(\mathcal{N}+1)P_{\mathcal{N}}^2(\tau_k)} \tag{20}$$

With the above steps, the OCP (13) is converted to the following NLP problem:

$$\begin{aligned} \min \mathcal{J} &= \frac{s_{\mathrm{T}}}{2}\sum\nolimits_{k=0}^{\mathcal{N}} \frac{w_k\left(\mathcal{Q}_{\mathrm{e}}(\mathbb{P}_k) + \beta(\mathbb{V}_k - v_{\mathrm{d}})^2\right)}{\mathbb{V}_k} \\ s.t.\ \sum\nolimits_{i=0}^{\mathcal{N}} D_{ki}\mathbb{V}_i &= \frac{s_{\mathrm{T}}}{2\mathbb{V}_k M}\left(\frac{\eta_{\mathrm{T}}\mathbb{P}_k}{\mathbb{V}_k} + \mathbb{B}_k - C_A\mathbb{V}_k^2 - F_R(\mathbb{S}_k)\right) \\ v_{\min} &\le \mathbb{V}_k \le v_{\max} \\ 0 &\le \mathbb{P}_k \le \mathcal{P}_{\max} \\ \mathcal{B}_{\lim} &\le \mathbb{B}_k < 0 \end{aligned} \tag{21}$$

The variables to be optimized in (21) include the vehicle speed $\mathbb{V}_k$, engine power $\mathbb{P}_k$, and brake force $\mathbb{B}_k$. This NLP is a high-dimensional (i.e., $3N+3$) sparse constrained problem, and is solved by the sequential quadratic programming (SQP) algorithm with the solver SNOPT [22].

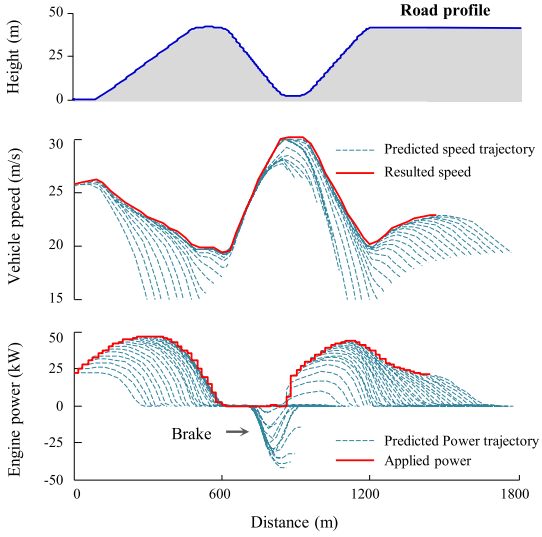

FIGURE 4. Speed planning results of the MPC algorithm including the predicted vehicle speed and engine power trajectories in each predictive horizon.

To better understand the MPC algorithm, an example is given in Fig. 4, which shows the optimized trajectories of vehicle speed and engine/brake power at each step. The actual applied power over the whole horizon and the resulting vehicle speed are highlighted by the red lines. It can be observed that the planned speed is dynamically changing to adapt to the road slopes.

IV. EQUIVALENT KINETIC-ENERGY AND FUEL CONVERSION (EKFC) ALGORITHM

Different from the MPC optimization in a preview horizon, in this Section we shorten the horizon and design a local optimization based speed planning algorithm called equivalent kinetic energy and fuel conversion (EKFC).

The concept of minimizing equivalent energy cost is inspired by the well-known energy management algorithm

of hybrid vehicles, i.e., equivalent consumption minimization strategy (ECMS) [16]. As mentioned in the introductory section, this algorithm optimizes the power allocation (not speed profile) between engine and motor relied on minimizing the sum of instantaneous fuel energy and battery energy. Since the vehicle speed is typically commanded by drivers or fixed by a given driving cycle, the vehicle kinetic energy is actually not involved in the optimization, as shown in Fig. 5. If we further extend the ECMS concept to the speed planning tasks, not only the fuel energy and battery energy but also the kinetic energy of vehicle body are all regarded as energy sources and can be allocated for better system efficiency. This concept was briefly introduced for the cruising control of conventional vehicles [17]. In this section, we leverage these concepts and extend them for fuel-saving speed planning of CAVs.

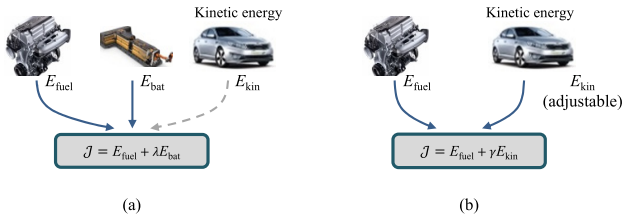

FIGURE 5. Available energy sources for energy management of hybrid vehicles and speed planning of conventional vehicles.

The EKFC algorithm to be designed explores the flexibility in vehicle speed by "tapping into" vehicle kinetic energy, similar to how the ECMS algorithm taps into the battery energy. In other words, the vehicle speed is the optimizable energy and the vehicle body acts as the buffer of kinetic energy. The difference is that when the vehicle kinetic energy is consumed, the vehicle speed slows down; while in the ECMS setting, when the battery energy is consumed, the battery SOC drops.

When a CAV runs on the slopes, the fuel-saving speed mainly depends on engine efficiency and aerodynamic drag. If the initial speed is over high, the economical operation would be to coast down to a lower speed, which avoids unnecessary high aerodynamic drag. In contrast, for an over low initial speed, the engine should accelerate the vehicle to avoid working at low load and low efficiency. The fuel-saving speed planning algorithm should pursue the best balance between better engine efficiency and lower aerodynamic drag. To achieve this goal, a local optimization problem is formulated below. It equivalently converts the kinetic energy to fuel and then minimizes the total energy consumption.

During a local short horizon Δt, the vehicle speed changes from v to $v + \Delta v$ with a fixed acceleration a, moving distance $\Delta s = v\Delta t$, engine power $\mathcal{P}_{\text{e}}$ and fuel consumption $\mathcal{Q}_{\text{e}}(\mathcal{P}_{\text{e}})\,\Delta t$. To minimize the consumed energy, the optimization problem is designed as

$$\begin{aligned}
\min_{\mathcal{P}_{\text{e}},\mathcal{B}}\ \mathcal{J} &= \lim_{\Delta s\to 0}\frac{\mathcal{Q}_{\text{e}}(\mathcal{P}_{\text{e}})\,\Delta t-\gamma\Delta E}{\Delta s}=\frac{\mathcal{Q}_{\text{e}}(\mathcal{P}_{\text{e}})}{v}-\gamma M\dot{v}\\
s.t.\ \dot{v} &= \frac{1}{M}\left(\frac{\eta_{\text{T}}\mathcal{P}_{\text{e}}}{v}+\mathcal{B}-C_A v^2-\mathcal{F}_R(s)\right)\\
\mathbb{C} &= \begin{bmatrix}\mathcal{P}_{\text{e}}\\ \mathcal{P}_{\max}-\mathcal{P}_{\text{e}}\\ \mathcal{B}-\mathcal{B}_{\lim}\\ -\mathcal{B}\end{bmatrix}\geq 0
\end{aligned}\tag{22}$$

where $\Delta E = Mv\dot{v}\Delta t$ is the change of kinetic energy, and C is the constraint vector of engine power and brake force.

The term γ in Eq. (22) is used to convert the consumed/increased kinetic energy to fuel; namely, it assigns a "price" to the kinetic energy. The price depends on the usable proportion of kinetic energy, which means how much kinetic energy can be used to overcome the unavoidable rolling resistance and gravity resistance [16]. Note that higher vehicle speed always corresponds to higher aerodynamic drag; thus the usable proportion of kinetic energy decreases and the price drops as the speed increases. In this paper, γ is designed as

$$\gamma(v)=\frac{\mathcal{F}_R(s)}{c_{\text{g}}\eta_{\text{T}}\eta_{\text{est}}\left(\mathcal{F}_R+C_A v^2\right)}\tag{23}$$

where c_{g} is the calorific value of gasoline; η_{est} is the estimated average engine efficiency and set empirically. In Eq. (23), we can see that a higher v leads to a lower γ, meaning more kinetic energy is wasted on aerodynamic drag and the price is cheaper.

When $v\in\mathbb{R}_v=(v_{\min},v_{\max})$, an open interval, the problem (22) is a nonlinear optimization problem with inequality constraints. The method of Lagrange multipliers is used to solve the problem, with the Lagrange function defined as

$$\begin{aligned}
&\min\ \mathcal{L}(\mathcal{P}_{\text{e}},\mathcal{B},\boldsymbol{\mu})\\
&\quad=\mathcal{J}+\boldsymbol{\mu}^{\text{T}}\mathbb{C}\\
&\quad=\frac{\mathcal{Q}_{\text{e}}(\mathcal{P}_{\text{e}})}{v}-\frac{\eta_{\text{T}}}{v}\gamma\mathcal{P}_{\text{e}}-\gamma\mathcal{B}+\boldsymbol{\mu}^{\text{T}}\mathbb{C}+\frac{\mathcal{F}_R}{\eta_{\text{T}}\eta_{\text{est}}c_{\text{g}}}
\end{aligned}\tag{24}$$

where $\boldsymbol{\mu}=[\mu_1,\mu_2,\mu_3,\mu_4]^{\text{T}}$ is the Lagrange multiplier vector. To achieve optimality, the Karush–Kuhn–Tucker (KKT) conditions should be satisfied [23], i.e.,

$$\nabla_{\mathcal{P}_{\text{e}},\mathcal{B}}\,\mathcal{L}=0,\quad \mu_i\,\mathbb{C}_i=0\tag{25}$$

For the brake force $\mathcal{B}$, we have

$$\begin{aligned}
&\frac{\partial\mathcal{L}}{\partial\mathcal{B}}=-\gamma+\mu_3-\mu_4=0\\
&\mu_3\mathcal{B}=0,\quad \mu_4(\mathcal{B}-\mathcal{B}_{\lim})=0
\end{aligned}\tag{26}$$

Since $\gamma>0$, $\mu_3-\mu_4\neq 0$. In addition, for $\forall\mathcal{B}\in[\mathcal{B}_{\lim},0]$, $\mathcal{B}$ and $\mathcal{B}-\mathcal{B}_{\lim}$ cannot be equal to zero simultaneously, thus either μ_3 or μ_4 should be 0. Considering the purpose of minimizing $\mathcal{L}$, we can infer that

$$\mathcal{B}^*\equiv 0,\quad \mu_4^*\equiv 0\tag{27}$$

which means that the brake operation will not be applied when $v \in (v_{\min}, v_{\max})$ because it always wastes energy.

For the engine power $\mathcal{P}_e$, the KKT conditions are

$$\begin{aligned} \frac{\partial \mathcal{L}}{\partial \mathcal{P}_e} &= \frac{\partial \mathcal{Q}_e(\mathcal{P}_e)}{v \partial \mathcal{P}_e} - \frac{\eta_T}{v}\gamma + \mu_1 - \mu_2 = 0 \\ \mu_1 \mathcal{P}_e &= 0, \quad \mu_2 (\mathcal{P}_{\max} - \mathcal{P}_e) = 0 \end{aligned} \tag{28}$$

If $\mathcal{P}_e \in (0, \mathcal{P}_{\max})$, then $\mu_1 = \mu_2 = 0$, and we get

$$\frac{\partial \mathcal{Q}_e(\mathcal{P}_e^*)}{\partial \mathcal{P}_e^*} - \frac{1}{\eta_{\text{est}} c_g} \frac{\mathcal{F}_R}{\mathcal{F}_R + C_A v^2} = 0 \tag{29}$$

Substituting the engine fuel model (8) into (29) results in

$$\mathcal{P}_e^* = -\frac{\kappa_1}{2\kappa_2} + \frac{\mathcal{F}_R(s)}{2\kappa_2 \eta_{\text{est}} c_g (\mathcal{F}_R + C_A v^2)} \tag{30}$$

This function establishes a direct mapping from the road slope $\theta(s)$ to the optimal engine power $\mathcal{P}_e^*$. Note that $\mathcal{L}$ is a convex quadratic function with regard to $\mathcal{P}_e$, i.e.,

$$\frac{\mathrm{d}^2 \mathcal{L}}{\mathrm{d}\mathcal{P}_e^2} = \frac{2\kappa_2}{v} > 0, \quad \mathcal{P}_e \geq 0 \tag{31}$$

Hence, when $v \in \mathbb{R}_v$, if the calculated $\mathcal{P}_e^* > \mathcal{P}_{\max}$, setting the output power $\bar{\mathcal{P}}_e = \mathcal{P}_{\max}$ achieves minimal $\mathcal{L}$ with $\mu_1 = 0$. If $\mathcal{P}_e^* < 0$, setting $\bar{\mathcal{P}}_e = 0$ with $\mu_2 = 0$. In addition, the constraints are also convex, thus the solution obtained from the necessary condition KKT is the optima of the problem (22).

When $v = v_{\max}$, the power to maintain $v_{\max}$ is defined as

$$\mathcal{P}_d(v_{\max}) = \frac{v_{\max}}{\eta_T}\left(C_A v_{\max}^2 + \mathcal{F}_R\right) \tag{32}$$

To avoid speeding, i.e., $v > v_{\max}$, the applied engine power $\bar{\mathcal{P}}_e$ or brake force $\bar{\mathcal{B}}$ is set as

$$\begin{cases} \bar{\mathcal{P}}_e = \min\left(\mathcal{P}_d(v_{\max}), \mathcal{P}_e^*, \mathcal{P}_{\max}\right), & \mathcal{P}_d(v_{\max}) \geq 0 \\ \bar{\mathcal{B}} = C_A v_{\max}^2 + \mathcal{F}_R(s), & \mathcal{P}_d(v_{\max}) < 0 \end{cases} \tag{33}$$

Similarly, if $v = v_{\min}$, the brake is not used and $\bar{\mathcal{P}}_e$ is set to

$$\bar{\mathcal{P}}_e = \max\left(\mathcal{P}_d(v_{\min}), \mathcal{P}_e^*, 0\right) \tag{34}$$

In summary, the engine/brake control rule of EKFC is designed as

$$\begin{aligned} \bar{\mathcal{P}}_e &= \begin{cases} \mathcal{P}_e^*, & v \in \mathbb{R}_v, \mathcal{P}_e^* \in (0, \mathcal{P}_{\max}) \\ \mathcal{P}_{\max}, & v \in \mathbb{R}_v, \mathcal{P}_e^* > \mathcal{P}_{\max} \\ 0, & v \in \mathbb{R}_v, \mathcal{P}_e^* < 0 \\ \min\left(\mathcal{P}_d(v_{\max}), \mathcal{P}_e^*, \mathcal{P}_{\max}\right), & v = v_{\max}, \mathcal{P}_d(v_{\max}) \geq 0 \\ \max\left(\mathcal{P}_d(v_{\min}), \mathcal{P}_e^*, 0\right), & v = v_{\min} \end{cases} \\ \bar{\mathcal{B}} &= C_A v_{\max}^2 + \mathcal{F}_R(s), \quad v = v_{\max}, \mathcal{P}_d(v_{\max}) < 0 \end{aligned} \tag{35}$$

Applying the control law (35) generates the fuel-saving speed at next step $v^*(t + \Delta t)$:

$$v^*(t + \Delta t) = v(t) + a|_{\bar{\mathcal{P}}_e, \bar{\mathcal{B}}} \Delta t \tag{36}$$

This speed planning algorithm is capable of generating both the optimal speed level and the throttle, brake, and transmission commands in a short local horizon.

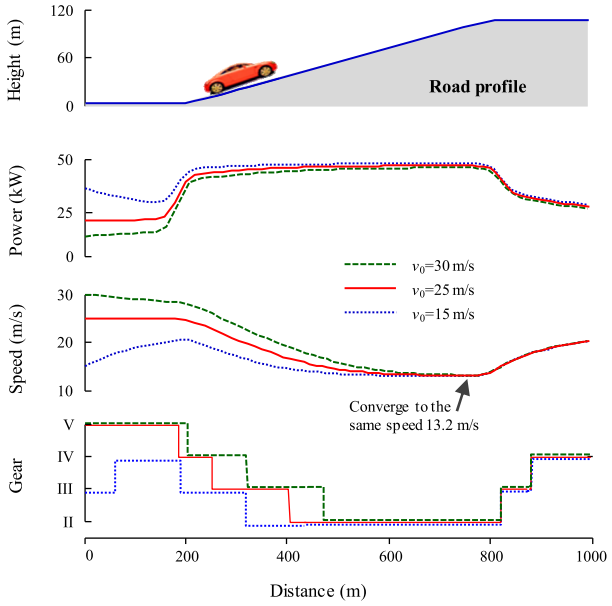

FIGURE 6. Speed planning results of the EKFC with different initial speeds on an uphill $\theta = 10°$.

An example of EKFC algorithm is given in Fig. 6. The task for the CAV is to cruise on a slope $\theta = 10°$ with an initial speed v_0 equal to 15, 25, and 30 m/s, respectively. The planned vehicle speed and engine(+)/brake(−) power are shown in Fig. 6. In the beginning stage, the algorithm selects to accelerate, keep the constant speed, and slow down for the three cases, respectively. On the up-slope, a key observation is that all of the vehicle speeds converge gradually to 13.2 m/s, along with the engine powers rising up and the vehicle speeds dropping down. The gear profile of AMT is also presented in Fig. 6. It downshifts to the second gear to climb uphill, and upshifts to the fourth gear for cruising on the flat road. We can see that these operations resemble the human drivers' behaviors in the real world.

As shown in Fig. 6, the speed profiles planned by the EKFC can adapt to the road slope. This result differs from the conventional cruising control (CC) system, which usually maintains a fixed vehicle speed regardless of road slopes. If the vehicle runs at a fixed speed v_d, the corresponding engine/brake power $\mathcal{P}_d$ is

$$\mathcal{P}_d(v) = \frac{v_d}{\eta_T}\left(C_A v_d^2 + \mathcal{F}_R(s)\right) \tag{37}$$

where $\mathcal{P}_d$ can be positive or negative. On a steep uphill or downhill, the demanded power may exceed the physical limits of engine ($\mathcal{P}_{\max}$) or braking system ($\mathcal{P}_{\min}$); thus the actual adopted power $\bar{\mathcal{P}}$ is set to

$$\bar{\mathcal{P}} = \begin{cases} \mathcal{P}_d, & v \in (v_d - \delta, v_d + \delta), \mathcal{P}_d \in [\mathcal{P}_{\min}, \mathcal{P}_{\max}] \\ \mathcal{P}_{\max}, & v < v_d - \delta \text{ or } \mathcal{P}_d > \mathcal{P}_{\max} \\ \mathcal{P}_{\min}, & v > v_d + \delta \text{ or } \mathcal{P}_d < \mathcal{P}_{\min} \end{cases} \tag{38}$$

where δ is the slack scalar for numerical stability. If $\mathcal{P}_d \in [\mathcal{P}_{min}, \mathcal{P}_{max}]$, the vehicle speed equals the given speed v_d. Otherwise, v will deviate from v_d. In this paper, we set this CC system as the benchmark for the proposed algorithms.

V. COMPARISON OF THE MPC AND EKFC ALGORITHMS

In this Section, we compare the performances of the near-global optimization based MPC algorithm and the local-optimization based EKFC algorithm. The result of CC system is also presented.

A. TESTING SCENARIOS

To quantitatively assess the fuel economy and computation efficiency of the two speed-planning algorithms, two testing scenarios are adopted: an 80 km urban expressway and a 180 km highway in a mountainous area of western China, as shown in Fig. 7. The two scenarios contain numerous natural slopes and are assumed to be suitable for performance evaluation.

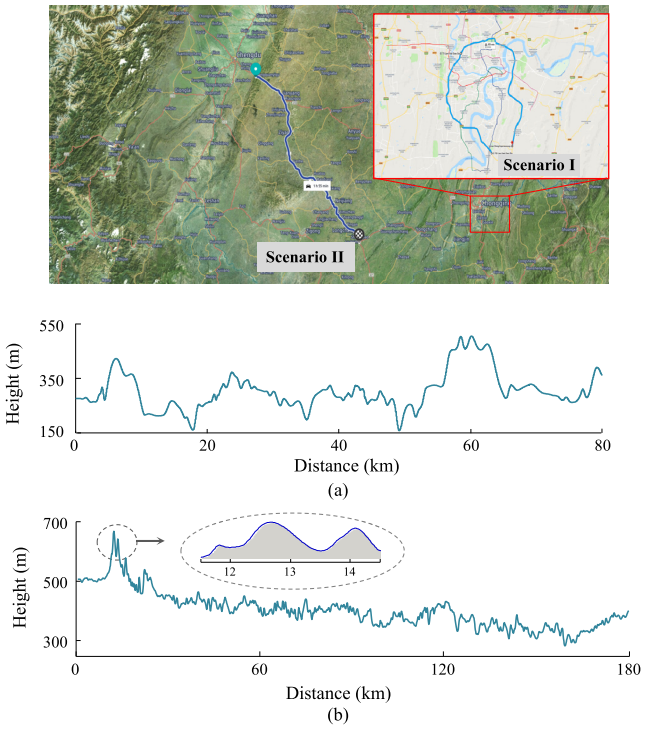

FIGURE 7. Testing scenarios for the speed-planning algorithms. (a) Scenario I: 80 km urban express road. (b) Scenario II: 180 km highway G76

B. SPEED PLANNING RESULTS

The MPC, EKFC, and CC methods are applied to the two scenarios. In Scenario I, the initial speed is set to 25.6 m/s. For the MPC algorithm, we set $s_T = 800$ meters, $\Delta s = 5$ meters, and $\beta = 0.01$. The resulted speed profile is shown in Fig. 8. To guarantee that the trip time of CC is same with the MPC, the target speed of CC is set to 23.60 m/s. For the EKFC, we select the speed range as [20, 29.8] m/s in order to achieve the same trip time. Note that the purpose of the same trip time is to achieve fair comparisons; thus the above tricks are used to adjust the trip time roughly. The planned speed and corresponding engine/brake power of EKFC and CC are also shown in Fig. 8.

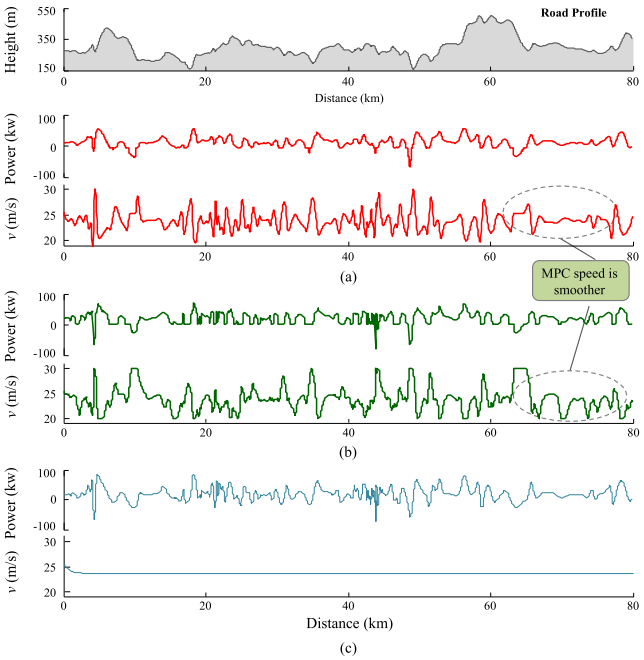

FIGURE 8. Fuel-oriented speed profiles planned by the MPC, EKFC, and CC algorithms for Scenario I. (a) MPC. (b) EKFC. (c) CC.

It can be observed that the engine power profiles of MPC and EKFC fluctuate in the similar trends in Fig. 8. Their engine operating points are shown in Fig. 9. Most of them fall within the high-efficiency area, i.e., 1500 $\sim$ 3500 rpm and 60 $\sim$ 150 Nm, denoted as the "ECO area." The resulted speed trajectories of MPC and EKFC also have the similar trends, but the former appears to be smoother than the latter. The CC system maintains a constant speed over the whole trip but has to use more aggressive operations with higher engine and brake powers.

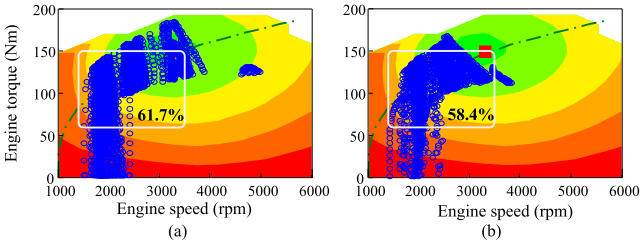

FIGURE 9. Engine operations of the MPC and EKFC in Scenario I. (a) MPC. (b) EKFC.

To further understand the engine and braking behaviors of the three methods, their power distributions are presented in Fig. 10, with the detailed values listed in Table 2. Both the EKFC and the MPC adopt more medium-level engine powers and fewer braking operations. While the CC takes

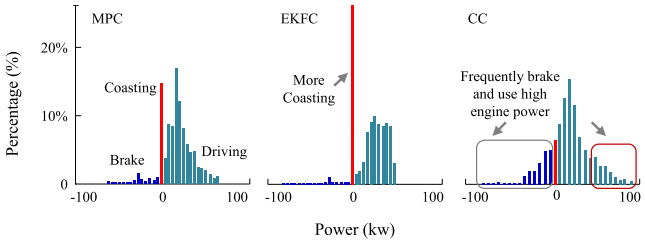

FIGURE 10. Engine/brake power distribution of the three methods in scenario I.

TABLE 2. Overview of the engine/brake power distribution in scenario I.

Method	Brake	Coast	Drive	Power in ECO Area	Power >60 kW
MPC	4.2%	13.9%	81.9%	61.7%	0.8%
EKFC	2.9%	27.6%	69.5%	58.4%	1.4%
CC	15.6%	5.8%	78.6%	50.7%	4.1%

the brake operations and the high engine powers (>60 kW) much more frequently compared with the others. We notice that the proportion of zero power in the EKFC is as high as 27.6%, meaning that it frequently operates in the coasting mode, especially when driving on the downhills.

TABLE 3. Fuel Consumption of the three algorithms on the 80/180 km highway.

	Method	MPC	EKFC	CC
Scenario I	Trip time (min)	56.5	56.7	56.5
	Consumed Fuel (kg)	5.22	5.27	5.67
	Fuel Saving Rate η_Q	-7.9%	-7.1%	-
Scenario II	Trip time (min)	120.5	120.6	120.5
	Consumed Fuel (kg)	11.67	11.92	13.21
	Fuel Saving Rate η_Q	-11.7%	-9.8%	-

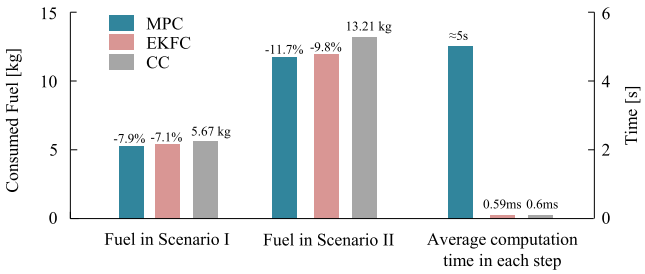

FIGURE 11. Comparison of the MPC, EKFC, and CC in fuel economy and computational efficiency.

C. FUEL ECONOMY AND COMPUTATIONAL LOAD

The fuel consumptions of the three methods in the two testing scenarios are reported in Table 3 and Fig. 11. Their trip times, as mentioned before, are roughly the same for a fair comparison by intentionally setting the speed level of CC and the speed bounds of EKFC. We can observe that both the MPC and EKFC algorithms outperform the fixed-speed CC system by about 7%-10% fuel-savings on the 80 km and 180 km highways. The EKFC achieves slightly worse fuel economy than the MPC, i.e., the fuel saving rate is lower by 1-2 percentage points.

Using a computer with an Intel i5 3.2 GHz CPU and the Matlab environment, we record the computation time of the three algorithms in each speed-planning loop. The average values are shown in Fig. 11. It can be found that the average computing time of EKFC and CC is about 0.6 milliseconds; the maximum is less than 2 milliseconds. Theoretically, the EKFC and CC have analytical speed-planning rules with only algebraic and logic operations. The MPC method solves the nonlinear constrained OCP in each speed-planning loop by the Legendre pseudo-spectral method. The computation time depends on the applied optimization algorithm as well as the problem complexity, including dimensions, nonlinearity, and constraints. The average computing time of the designed MPC algorithm is about 5 seconds for each step. Note that the predictive horizon is 800 meters, which can be translated to 40s at 20 m/s. In general, the nonlinear optimization based MPC naturally has much heavier computing load than the EKFC and CC with analytical solutions, even though the computation efficiency of MPC may be further improved by, e.g., using more advanced algorithms.

VI. DISCUSSIONS

In this Section, we qualitatively discuss the mechanism of the different fuel economies between the MPC and EKFC. Generally, the fuel economy of speed planning algorithms mainly depends on the following two factors:

1) Ability of "slope adaptation." For example, the EKFC matched the speed level with the road topology well as shown in Fig. 6. The CC system, however, maintains a constant speed and is not adaptive at all. The lack of slope-adaption led to inappropriate speed, inefficient engine operations, and unnecessary braking, thus ending up with the poor fuel economy.
2) Ability of "prediction," which can plan vehicle speed based on future information. An example is given in Fig. 12; the MPC reduces the engine power earlier at the end of the first uphill, and avoids braking operation at the subsequent downhill; while the EKFC suffers from a mild brake due to the unawareness of the upcoming downhill.

To understand the fuel-saving results, we qualitatively summarize the two abilities of the three methods in Table 4. The slope adaptation abilities are sorted as EKFC $\approx$ MPC $>$ CC. Note that the MPC is slightly restrained by the penalty on speed deviation. The prediction abilities follow the order of MPC $>$ EKFC $=$ CC, i.e., the EKFC and CC forfeit prediction ability completely. In summary, the performance in these two abilities dominates the

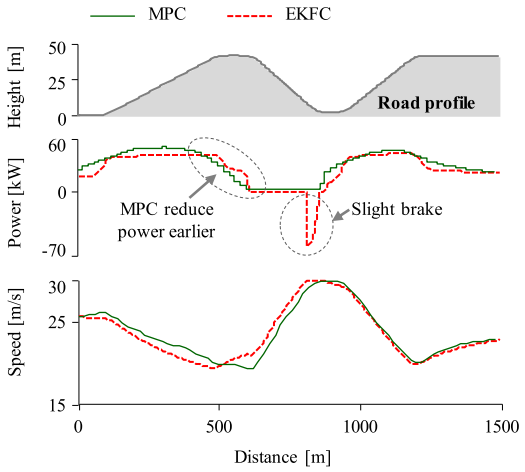

FIGURE 12. Demonstration of the prediction ability of MPC.

TABLE 4. Characteristics of the designed speed planning methods.

Controller	MPC	EKFC	CC
Slope adaptation	★	★★	No
Prediction	★★	No	No
Fuel economy	★★	★★	★
Computation efficiency	★	★★	★★

fuel-saving potential, i.e., the MPC achieved the best fuel economy, the EKFC is close to but slightly worse than the MPC, and they perform better than the CC strategy. In real applications, designers can select the proper method based on their preference for fuel economy or computational efficiency.

VII. CONCLUSIONS

This paper designed and compared the receding-horizon optimization based MPC algorithm and the local optimization based EKFC algorithm to achieve fuel-saving speed planning for automated vehicles. The MPC method solved the optimal speed profile considering the previewed road slopes in the future finite horizon. The formulated fuel-optimal problem was solved by the Legendre pseudo-spectral method numerically. The EKFC algorithm considered the vehicle kinetic energy an admissible power source that can be tapped into fuel consumption; it minimized the sum of fuel energy and kinetic energy and then generated the fuel-saving speed level. We compared the two speed-planning strategies by numerical simulations. The results showed that the MPC and EKFC achieved about 7% fuel reduction than the constant-speed cruising control system in the two testing scenarios. The fuel economy of EKFC is close to but slightly worse than the MPC method, i.e., consumed about 2% more fuel. One major benefit of the EKFC is that it has negligible computation load due to its analytical speed-planning laws, which is more flexible than the nonlinear optimization based MPC for online implementation.

REFERENCES

[1] L. D. Burns, "Sustainable mobility: A vision of our transport future," *Nature*, vol. 497, no. 7448, pp. 181–182, 2013.
[2] J. N. Barkenbus, "Eco-driving: An overlooked climate change initiative," *Energy Policy*, vol. 38, no. 2, pp. 762–769, 2010.
[3] S. Xu, S. E. Li, H. Peng, B. Cheng, X. Zhang, and Z. Pan, "Fuel-saving cruising strategies for parallel HEVs," *IEEE Trans. Veh. Technol.*, vol. 65, no. 6, pp. 4676–4686, Jun. 2016.
[4] F. Mensing, E. Bideaux, R. Trigui, and H. Tattegrain, "Trajectory optimization for eco-driving taking into account traffic constraints," *Transp. Res. D, Transp. Environ.*, vol. 18, pp. 55–61, Jan. 2013.
[5] A. E. Atabani, I. A. Badruddin, S. Mekhilef, and A. S. Silitonga, "A review on global fuel economy standards, labels and technologies in the transportation sector," *Renew. Sustain. Energy Rev.*, vol. 15, no. 9, pp. 4586–4610, Dec. 2011.
[6] S. E. Li and H. Peng, "Strategies to minimize the fuel consumption of passenger cars during car-following scenarios," *Proc. Inst. Mech. Eng. D, J. Automobile Eng.*, vol. 226, no. 3, pp. 419–429, 2012.
[7] S. E. Li, S. Xu, X. Huang, B. Cheng, and H. Peng, "Eco-departure of connected vehicles with V2X communication at signalized intersections," *IEEE Trans. Veh. Technol.*, vol. 64, no. 12, pp. 5439–5449, Dec. 2015.
[8] B. Asadi and A. Vahidi, "Predictive cruise control: Utilizing upcoming traffic signal information for improving fuel economy and reducing trip time," *IEEE Trans. Control Syst. Technol.*, vol. 19, no. 3, pp. 707–714, May 2011.
[9] A. B. Schwarzkopf and R. B. Leipnik, "Control of highway vehicles for minimum fuel consumption over varying terrain," *Transp. Res.*, vol. 11, no. 4, pp. 279–286, 1977.
[10] E. Hellström, M. Ivarsson, J. Åslund, and L. Nielsen, "Look-ahead control for heavy trucks to minimize trip time and fuel consumption," *Control Eng. Pract.*, vol. 17, pp. 245–254, Feb. 2009.
[11] S. E. Li *et al.*, "Performance enhanced predictive control for adaptive cruise control system considering road elevation information," *IEEE Trans. Intell. Vehicles*, vol. 2, no. 3, pp. 150–160, Sep. 2017.
[12] H. Lim, W. Su, and C. C. Mi, "Distance-based ecological driving scheme using a two-stage hierarchy for long-term optimization and short-term adaptation," *IEEE Trans. Veh. Technol.*, vol. 66, no. 3, pp. 1940–1949, Mar. 2017.
[13] A. D. Ames, J. W. Grizzle, and P. Tabuada, "Control barrier function based quadratic programs with application to adaptive cruise control," in *Proc. IEEE 53rd Annu. Conf. Decision Control (CDC)*, Dec. 2014, pp. 6271–6278.
[14] M. A. S. Kamal, M. Mukai, J. Murata, and T. Kawabe, "Ecological vehicle control on roads with up-down slopes," *IEEE Trans. Intell. Transp. Syst.*, vol. 12, no. 3, pp. 783–794, Sep. 2011.
[15] Y. Wang and S. Boyd, "Fast model predictive control using online optimization," *IEEE Trans. Control Syst. Technol.*, vol. 18, no. 2, pp. 267–278, Mar. 2010.
[16] C. Musardo, G. Rizzoni, Y. Guezennec, and B. Staccia, "A-ECMS: An adaptive algorithm for hybrid electric vehicle energy management," *Eur. J. Control*, vol. 11, no. 4, pp. 509–524, 2005.
[17] S. Xu, S. E. Li, B. Cheng, and K. Li, "Instantaneous feedback control for a fuel-prioritized vehicle cruising system on highways with a varying slope," *IEEE Trans. Intell. Transp. Syst.*, vol. 18, no. 5, pp. 1210–1220, May 2017.
[18] G. Genta, *Motor Vehicle Dynamics: Modeling and Simulation*. London, U.K.: World Scientific, 1997, pp. 205–274.
[19] S. Xu, S. E. Li, K. Deng, S. Li, and B. Cheng, "A unified pseudospectral computational framework for optimal control of road vehicles," *IEEE/ASME Trans. Mechatronics*, vol. 20, no. 4, pp. 1499–1510, Aug. 2015.
[20] G. Elnagar, M. A. Kazemi, and M. Razzaghi, "The pseudospectral Legendre method for discretizing optimal control problems," *IEEE Trans. Autom. Control*, vol. 40, no. 10, pp. 1793–1796, Oct. 1995.
[21] I. M. Ross and F. Fahroo, "Pseudospectral knotting methods for solving nonsmooth optimal control problems," *J. Guid., Control, Dyn.*, vol. 27, no. 3, pp. 397–405, 2004.
[22] P. E. Gill, W. Murray, and M. A. Saunders, "SNOPT: An SQP algorithm for large-scale constrained optimization," *SIAM Rev.*, vol. 47, no. 1, pp. 99–131, 2005.
[23] H. W. Kuhn, "Nonlinear programming: A historical view," in *Traces and Emergence of Nonlinear Programming*, G Giorgi and T. Kjeldsen, Eds. Basel, Switzerland: Birkhäuser, 2014, pp. 393–414.

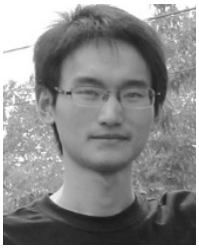

SHAOBING XU received the Ph.D. degree in mechanical engineering from Tsinghua University, Beijing, China, in 2016.

He is currently a Post-Doctoral Research Fellow with the Department of Mechanical Engineering, University of Michigan, Ann Arbor. His research interests include autonomous vehicle, vehicle motion control, optimal control theory, decision making, and path planning for automated vehicles. He was a recipient of the Outstanding Ph.D. Dissertation Award of Tsinghua University, the First Prize of the Chinese Fourth Mechanical Design Contest, and the First Prize of the 19th Advanced Mathematical Contest.

HUEI PENG received the Ph.D. degree in mechanical engineering from the University of California, Berkeley, in 1992.

He is currently a Professor with the Department of Mechanical Engineering, University of Michigan, and the Director of Mcity. He is a ChangJiang Scholar with the Tsinghua University of China. His research interests include adaptive control and optimal control, with emphasis on their applications to vehicular and transportation systems. His current research focuses include design and control of electrified vehicles and connected/automated vehicles. He is a fellow of SAE and ASME.